ELSEVIER

Contents lists available at ScienceDirect

Organic Electronics

journal homepage: www.elsevier.com/locate/orgel





Evidence for long drift carrier lifetimes in $[Fe(Htrz)_2(trz)](BF_4)$ plus polyaniline composites

Esha Mishra ^{a,*}, Thilini K. Ekanayaka ^a, Kayleigh A. McElveen ^b, Rebecca Y. Lai ^b, Peter A. Dowben ^a

a Department of Physics and Astronomy, Theodore Jorgensen Hall, 855 North 16th Street, University of Nebraska-Lincoln, Lincoln, NE, 68588-0299, USA

ARTICLE INFO

Keywords: Fe(Htrz)₂(trz)](BF₄) Spin crossover molecule Polyaniline

ABSTRACT

An effort has been made to determine the majority carrier and drift carrier lifetimes in the promising spin crossover molecule $[Fe(Htrz)_2(trz)](BF_4)$ (where Htrz=1H-1,2,4-triazole) plus polyaniline composite. The current voltage and capacitance voltage characteristics of the $[Fe(Htrz)_2(trz)](BF_4)$ plus polyaniline composite were studied at both the low spin state at T=320 K and the high spin state at T=380 K. In these composites, the drift carrier lifetimes are in excess of microseconds, and there are indications that the majority carriers are holes. While the drift carrier lifetime is much lower when the $[Fe(Htrz)_2(trz)](BF_4)$ plus polyaniline composite is in the low spin state, there are indications that for at least one polyaniline composite, the carrier mobility is much higher in the low spin state so that the mobility is consistent with the higher conductivity of the low spin state.

1. Introduction

When a complex compound involving transition metals with usually 3d⁴-3d⁷ electronic configuration, is thermally induced, it undergoes a change in spin multiplicity, and are thus known as spin crossover compounds [1]. In addition to responding to changing temperature, the spin state, in spin crossover molecules, also can change in response to an external stimuli such as pressure, light or electric field [2–8]. Such spin crossover molecules could be an important addition to molecular electronics as they provide a facile read mechanism in combination with an organic ferroelectric [9] because the change in spin state is often associated with a change in conductance. In recent years, spin crossover molecules have been successfully utilized, in combination with organic ferroelectrics, to fabricate non-volatile voltage controlled memory devices [9-11]. Some of the important criteria for the fabrication of molecular devices based on spin crossover molecules have been outlined [9], but it is very clear that the high resistance of most spin crossover molecular films is a key impediment to a competitive molecular nonvolatile memory devices.

A recent study on [Fe(Htrz)₂(trz)](BF₄) (where Htrz = 1H-1,2,4-triazole) demonstrated that the addition of the semiconducting polymer polyaniline leads to a low on state resistance [12]. This resistance well below 1 Ω cm makes [Fe(Htrz)₂(trz)](BF₄) plus polyaniline composites

potentially very suitable for competitive molecular memory applications [9]. [Fe(Htrz)₂(trz)](BF₄) (where Htrz = 1H-1,2,4-triazole) [12–20,22,25] is among the more commonly studied spin crossover molecules based on iron [12–25], with a spin transition temperature somewhat above room temperature (i.e. 330–380 K) that is accompanied by a conductance change. Some electrical measurements on [Fe(Htrz)₂(trz)] (BF₄) have revealed that the conductivity in the low spin state is higher in comparison to the high spin state [19,20,22,25], which has been attributed to the lower activation barrier in the low spin state [20]. Just the same it should be noted that there are other studies that indicate the reverse, that is to say that the conductivity in the high spin state is higher than the low spin state [12,15] suggesting that [Fe(Htrz)₂(trz)](BF₄), may have multiple thin film phases.

Considering the promise of [Fe(Htrz)₂(trz)](BF₄) plus polyaniline for organic device applications [12], it should be noted that polyaniline can be synthesized into three different oxidation states: pernigraniline, leucoemeraldine, and emeraldine (half-oxidized). Of these different polyanilines, the emeraldine form is environmentally and chemically stable, and is conductive in the salt form but not in the base form [26]. The emeraldine base form is less conductive than the salt form, with a resistance greater than $10^{10}~\Omega$ cm [26], thus essentially dielectric. Yet the emeraldine base form of polyaniline can be protonated through doping, with a protonic acid, rendering it more conductive [27,28].

E-mail address: emishra@huskers.unl.edu (E. Mishra).

^b Department of Chemistry, Hamilton Hall, University of Nebraska-Lincoln, Lincoln, NE, 68588-0304, USA

^{*} Corresponding author.

Thus the more insulating polyaniline polymers are converted to the conductive form by introducing charge transfer complexes within the electron donors and electron acceptors inside the polymer chain [27–29].

While composites of [Fe(Htrz)₂(trz)](BF₄) with semiconducting polymer polyaniline (whose structures are shown in Fig. 1) has an atypically low on state resistance, as just noted [12], not much else is known about the transport properties of these composites. We, therefore, studied the current-voltage, capacitance-voltage, and transfer characteristics of the combination of [Fe(Htrz)₂(trz)](BF₄) plus polyaniline composite at both the low spin state (at $T=320~{\rm K}$) and the high spin state (at $T=380~{\rm K}$).

2. Methodology

Two types of polyaniline were used in this study to show the contrast between the different routes to doping polyaniline. Polyaniline 1 was a 5000 g/mol polyaniline synthesized in-house. This polyaniline 1 was synthesized into the emeraldine salt form using HCl and was not undoped into the base form and then redoped with acid. 10 mL of 1 M hydrochloric acid (HCl) containing 0.25 M ammonium persulfate was added to 30 mL of 0.25 M aniline in water at 0 °C, as described elsewhere [30]. The mixture was stirred for 6 h and was allowed to sit overnight at room temperature. The resulting dark green precipitate was collected and then washed thoroughly with 1 M HCl, ethanol, and water.

Polyaniline **2** was a polyaniline that was synthesized from the purchased polyaniline emeraldine base (Sigma Aldrich 556459-25G) and was further doped with p-toluene sulfonic acid to the emeraldine salt form, this polyaniline emeraldine base was converted to the salt form using 0.5 M p-toluene sulfonic acid [31,32]. While HCl is often used for doping, it has a tendency to form side reactions and has low stability. P-toluene sulfonic acid was used instead because sulfonic acid dopants improve processibility, yield, and electrical properties [29].

[Fe(Htrz)₂(trz)](BF₄) was synthesized as reported in Kroeber et al. [14]. To obtain [Fe(Htrz)₂(trz)](BF₄) plus polyaniline 1/polyaniline 2 composite solutions, 5 ± 1 mg of [Fe(Htrz)₂(trz)](BF₄) plus 5 ± 1 mg of either polyaniline 1 or polyaniline 2 were mixed with 4 ml of distilled water. Composites rich in polyaniline (i.e. close to a 1:1 ratio of SCO to polyaniline) are seen to have the highest conductance, although less

Fig. 1. (a) The schematic structure of $[Fe(Htrz)_2(trz)](BF_4)$. (b) The schematic structure of polyaniline (PANI). Hydrogen is omitted for clarity.

impressive on to off conductance ratios compared to composites more rich in [Fe(Htrz)₂(trz)](BF₄) [12].

To make the films, $[Fe(Htrz)_2(trz)](BF_4)$ plus polyaniline $1/polyaniline\ 2$ composite solutions were drop casted on prepatterned electrodes from Fraunhofer Institute for Photonic Microsystems (IPMS), designed for organic field effect transistor (OFET) fabrication. These $[Fe\ (Htrz)_2(trz)](BF_4)$ plus polyaniline composite films were dried to be free of solvent prior to the device measurements. The current-voltage, capacitance-voltage characteristics, and transistor measurements were performed on an OFET from Fraunhofer Institute for Photonic Microsystems (IPMS). The data were collected using 4200A-SCS parameter Analyzer and cryogenic lakeshore probe station, in the absence of illumination.

3. Results and discussion

Fig. 2 shows the voltage-dependent current characteristics of [Fe $(Htrz)_2(trz)](BF_4)$ plus polyaniline. As seen in both Fig. 2a and b, for both [Fe(Htrz)_2(trz)](BF_4) plus polyaniline 1 and polyaniline 2, the conductance of the high spin state (at T=380~K) is lower than the low spin state (at T=320~K), as has been seen in [Fe(Htrz)_2(trz)](BF_4) alone [19,20]. The difference in conductivity is attributed to polyaniline 1 being synthesized as the emeraldine salt form, while polyaniline 2 was obtained by converting the emeraldine base to the salt form via doping with p-toluenesulfonic acid. The optimal degree of doping of the polyaniline is $\sim 20\%$ [33], but it is challenging to control the extent of doping during the conversion process. Thus, there is a potential for under- or over-doping, which could lower the conductivity of the polymer [33]. Over-oxidation of the polymer could also lead to a reduction in the conductivity [34]. Other potential contributors to the noted difference

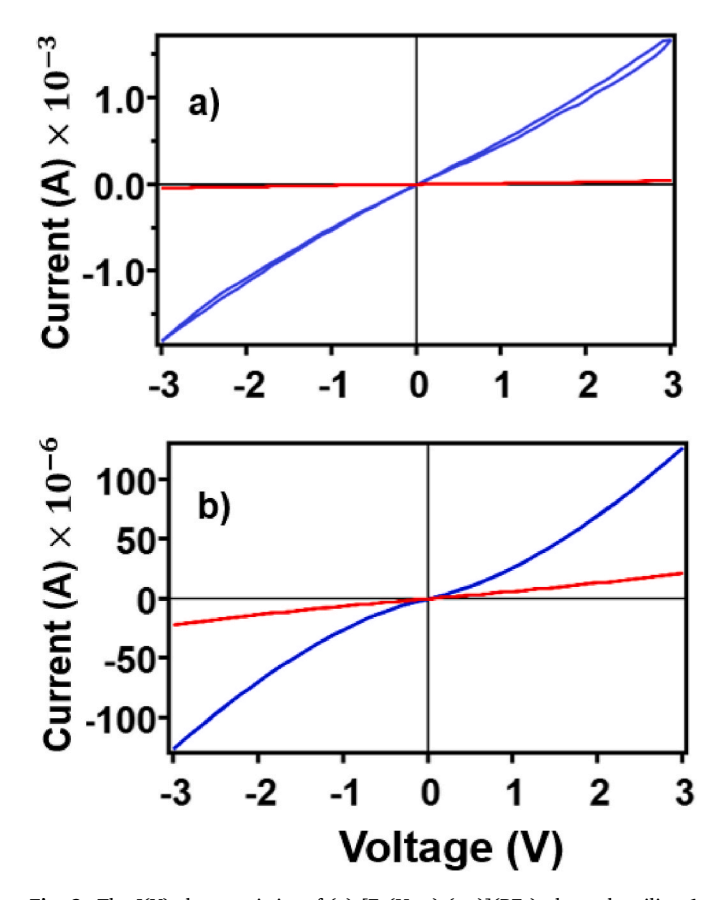


Fig. 2. The I(V) characteristics of (a) $[Fe(Htrz)_2(trz)](BF_4)$ plus polyaniline 1 compared to (b) $[Fe(Htrz)_2(trz)](BF_4)$ plus polyaniline 2. Blue color refers to the measurement at T=320 K (the low spin state) and red color refers to the measurement at T=380 K (the high spin state).

include the differences in size and morphology, and the arrangement of polymer chains between the two polyanilines used in this study [35,36]. As noted above, the high conductance is seen with polyaniline to [Fe $(Htrz)_2(trz)](BF_4)$ ratios close to close to a 1:1 [12] although as seen here, this may depend on the choice of polyaniline.

The comparison of I(V) characteristics of [Fe(Htrz)₂(trz)](BF₄) plus polyaniline **1** with [Fe(Htrz)₂(trz)](BF₄) plus polyaniline **2** elucidates the fact that the conductance at the low spin state is significantly higher for [Fe(Htrz)₂(trz)](BF₄) plus polyaniline **1** than [Fe(Htrz)₂(trz)](BF₄) plus polyaniline **2**. In other words, the on-state resistance of the low spin state is smaller for [Fe(Htrz)₂(trz)](BF₄) plus polyaniline **1** than [Fe (Htrz)₂(trz)](BF₄) plus polyaniline **2**. The higher conductance before heating in comparison to after heating has been observed in other spin crossover systems such as [Fe(HB(pz)₃)₂] [37].

The capacitance versus voltage, C(V) measurements at 1 MHz for [Fe (Htrz)₂(trz)](BF₄) plus polyaniline are shown in Fig. 3a and b. In both [Fe(Htrz)₂(trz)](BF₄) plus polyaniline 1 and [Fe(Htrz)₂(trz)](BF₄) plus polyaniline 2 composites, the capacitance at the high spin state is greater than the capacitance at the low spin state. This result suggests that the amount of charge trapping is greater in the high spin state in comparison to the low spin state. The nature of the C(V) curve for the low spin state in both cases of [Fe(Htrz)₂(trz)](BF₄) plus polyaniline 1 and [Fe (Htrz)₂(trz)](BF₄) plus polyaniline 2 suggests that with the increase in voltage the amount of charge trapping decreases. The phenomenon of charge trapping is also supported by the fact that the trapped charges have some role to play in inducing the hysteresis in capacitance-voltage characteristics [38] as observed in Fig. 3.

From the capacitance versus voltage and the current versus voltage data above, we can estimate the drift carrier lifetime. The conductance for the measurements involving low frequency is defined as [39–45]:

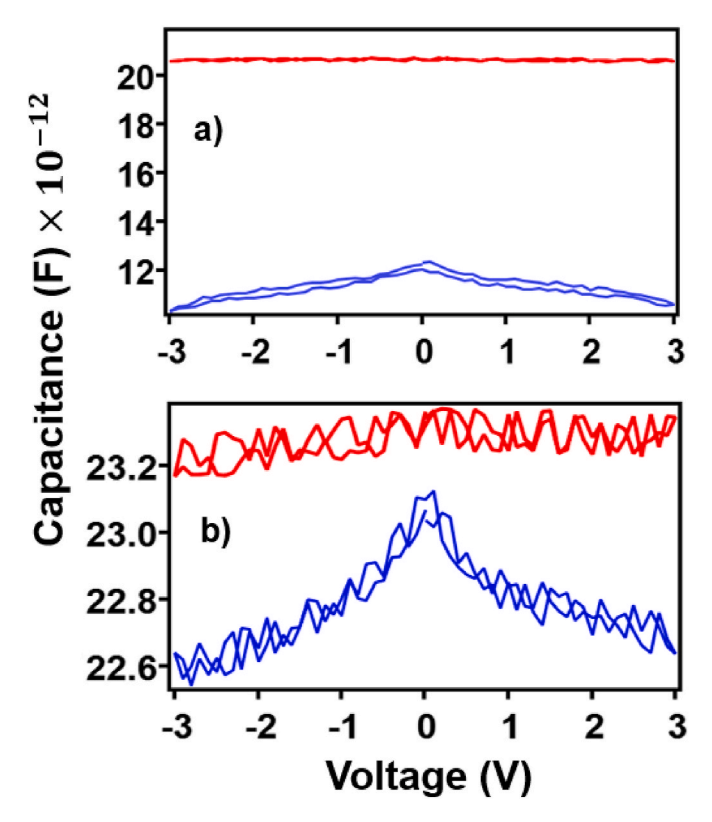


Fig. 3. The capacitance versus voltage, C(V), characteristics of (a) [Fe $(Htrz)_2(trz)](BF_4)$ plus polyaniline 1 *versus* (b) [Fe $(Htrz)_2(trz)](BF_4)$ plus polyaniline 2. Blue color refers to the measurement at T=320~K (the low spin state) and red color refers to the measurement at T=380~K (the high spin state).

$$G_0 = \frac{dI}{dV} \tag{1}$$

and the diffusion capacitance, C_D , is given as [39–45]:

$$C_D = \frac{G_0}{\omega \sqrt{2}} \left(\sqrt{1 + \omega^2 \tau^2} - 1 \right)^{\frac{1}{2}}$$
 (2)

Here, ' τ ' is the carrier lifetime and ' ω ' = 2 π f is the angular frequency, f being the frequency. Rewriting equation (2), we obtain the expression for carrier lifetime τ as:

$$\tau = \frac{\left(\left(\left(\frac{C_D\omega\sqrt{2}}{G_0}\right)^2 + 1\right)^2 - 1\right)^{\frac{1}{2}}}{C_0}$$
(3)

As shown in Fig. 4a and b, the carrier lifetime of the high spin state is higher in comparison to the carrier lifetime of the low spin state for both of the $[Fe(Htrz)_2(trz)](BF_4)$ plus polyaniline 1 and $[Fe(Htrz)_2(trz)](BF_4)$ plus polyaniline 2. The dipole changes across the spin transition and higher carrier lifetime of the high spin state in comparison to the low spin state could possibly be due to the reorientation of the molecular electrostatic dipoles at a higher temperature or the spin configuration. The larger intrinsic electric field associated with the larger dipole in the high spin state suppresses recombination. Additionally, exciton recombination could be suppressed because of forbidden spin flip transitions. Whatever the reasons, carrier lifetime behavior is significantly higher in the high spin state than the low spin state for $[Fe(Htrz)_2(trz)](BF_4)$ plus polyaniline, as observed in Fig. 4.

As shown in Fig. 5, the drain current for $[Fe(Htrz)_2(trz)](BF_4)$ plus polyaniline, in the low spin state (at T=320 K) is higher than the high spin state (at T=380 K) which is consistent with the I(V) characteristics

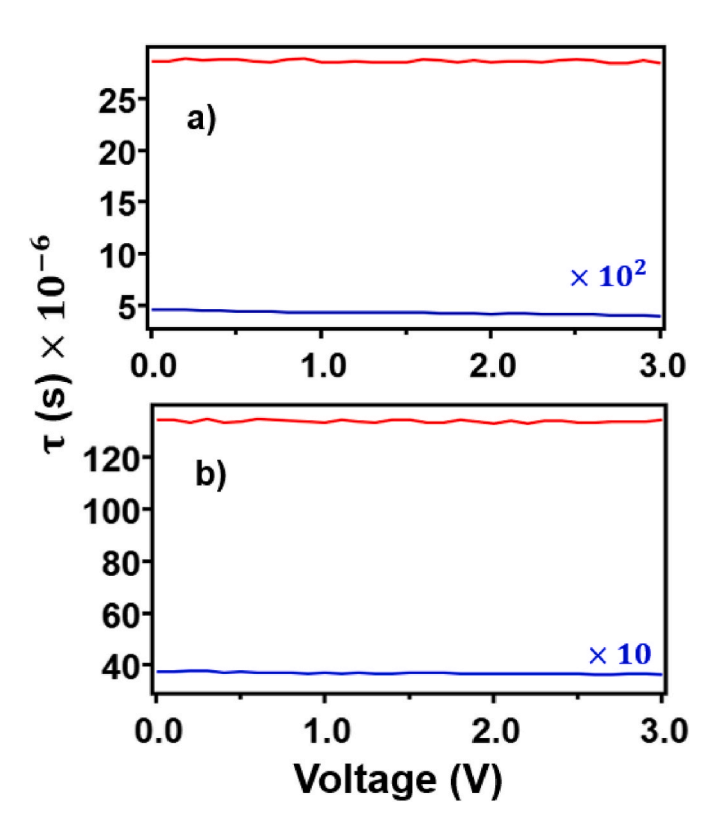


Fig. 4. The carrier lifetime versus voltage of (a) $[Fe(Htrz)_2(trz)](BF_4)$ plus polyaniline **1** compared with (b) $[Fe(Htrz)_2(trz)](BF_4)$ plus polyaniline **2**. Blue color refers to the measurement at T=320 K (the low spin state) and red color refers to the measurement at T=380 K (the high spin state). The carrier lifetime at T=320 K was scaled as labeled.

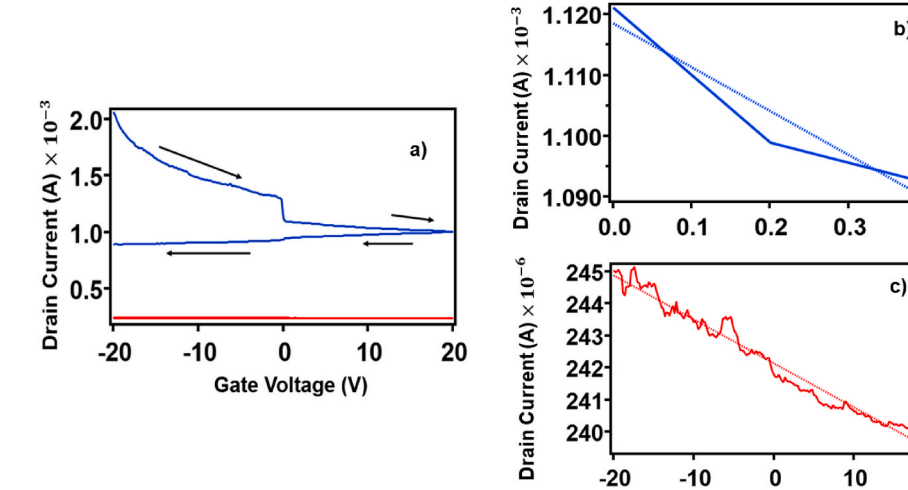


Fig. 5. a) The source to drain current transfer characteristics of Fe(Htrz)₂(trz)](BF₄) plus polyaniline 1. Source to drain currents are plotted for gate voltages ranging from -20 V to +20 V at 15 V source voltage. The blue and red curves indicate the drain current at T = 320 K and T = 380 K respectively. Drain current versus gate voltage of Fe(Htrz)2(trz)](BF4) plus polyaniline 1 at b) low spin state (T = 320 K) and c) high spin state (T = 380 K). The solid line represents the actual data points whereas the dashed line represents the slope of the line in b) and c).

shown in Fig. 2a for Fe(Htrz)₂(trz)](BF₄) plus polyaniline 1. The shape of the drain current versus gate voltage curve in Fig. 5 indicates that the hole and electron charge trapping is not equal. As the largest source to drain currents are seen with negative gate voltages and decrease with positive gate voltages, as shown by the drain current versus gate voltage shown in Fig. 5b and c. This suggests that the hole carrier concentration is greater than the electron carrier concentration. Although unproven, the nature of the curve in Fig. 5 suggests that the thin films of Fe (Htrz)₂(trz)](BF₄) plus polyaniline are p-type and the majority carriers are holes. This is consistent with the suggestion that Fe(II) spin crossover complexes tend towards cationic [46].

As shown in Fig. 5b and c, the magnitude of the slope of drain current versus gate voltage of Fe(Htrz)₂(trz)](BF₄) plus polyaniline 1 at the low spin state (at T=320 K) and at the high spin state (at T=380 K) is in order of ${\sim}10^{-5}$ and ${\sim}10^{-7}$ respectively. The formula for obtaining the field effect mobility ' μ ' used in the prior study [47] is given by:

$$\mu = \frac{L}{WC_i V_{ds}} \frac{dI_{ds}}{dV_g} \tag{4}$$

where, the transistor parameters 'L' is the channel length, 'W' is the channel width and 'C_i' is the gate dielectric capacitance per unit area.

Considering all the transistor parameters to be constant at the high spin state and the low spin state for Fe(Htrz)₂(trz)](BF₄) plus polyaniline 1, the field effect mobility becomes proportional to the slope of drain current versus the gate voltage. Since the magnitude of the slope of the low spin state (at T = 320 K) is higher than the high spin state (T = 380K) for Fe(Htrz)₂(trz)](BF₄) plus polyaniline 1, the mobility for low spin state (T = 320 K) of Fe(Htrz)₂(trz)](BF₄) plus polyaniline 1 is greater. For Fe(Htrz)₂(trz)](BF₄) plus polyaniline 1: $(\mu_{T=320 \text{ K}}) \propto 10^{-5}$, $(\mu_{T=380 \text{ K}}) \propto$ 10^{-7} .

Thus the carrier mobility of Fe(Htrz)₂(trz)](BF₄) plus polyaniline 1 at the high spin state (T = 380 K) is significantly smaller in comparison to the low spin state (T = 320 K) i.e., $\mu_{T=320~K} > \mu_{T=380~K}$, yet, as shown in Fig. 4a, in the case of Fe(Htrz)₂(trz)](BF₄) plus polyaniline 1, the carrier lifetime at the low spin state (T = 320 K) is much smaller in comparison to the high spin state (T = 380 K). So while the drift carrier lifetime in the high spin state is nearly 3×10^3 times larger than the drift carrier lifetime in the low spin state, higher mobilities may more than compensate for low drift carrier lifetime. For the case of Fe(Htrz)₂(trz)] (BF₄) plus polyaniline 2, analysis of the transistor curves in a like manner has, so far, not been possible.

Unlike drift carrier lifetime which measures every charge carrier, transistor mobility tends to be dominated by the most mobile carriers. The much higher transistor mobility seen here suggests that the conductivity in the low spin state should be higher than the high spin state. As shown in Fig. 2a, the conductance at the high spin state is lower than the low spin state for Fe(Htrz)₂(trz)](BF₄) plus polyaniline 1 and consistent with the lower carrier mobility of Fe(Htrz)2(trz)](BF4) plus polyaniline 1 in the high spin state. In fact, the complex interplay between carrier mobility and carrier lifetime, which both contribute to the overall conductance may explain why some [Fe(Htrz)₂(trz)](BF₄) thin films have the conductivity in the low spin state higher in comparison to the high spin state [19,20,22,25], while other studies have the conductivity in the high spin state is higher than the low spin state [12,15]. The complexity of this interplay between lifetime and mobility is brought into clarity by noting that the drift carrier lifetime of Fe (Htrz)₂(trz)](BF₄) alone (without polyaniline) could be as high as 100 ms. This is a much larger carrier lifetime than noted here (Fig. 4), but for Fe(Htrz)₂(trz)](BF₄) thin films, without the addition of polyaniline, the conductivity is considerably less [12].

4. Conclusion

Gate Voltage (V)

b)

0.4

20

We have studied the voltage-controlled transport properties of the combination of [Fe(Htrz)₂(trz)](BF₄) plus polyaniline composite at both the low spin state (at T = 320 K) and the high spin state (at T = 380 K). The conductance at low spin state (at T = 320 K) was higher than the conductance at the high spin state (at T = 380 K) for both the polyaniline (polyaniline 1 and polyaniline 2) plus [Fe(Htrz)₂(trz)](BF₄) composites. It is clear that the conductance changes expected with [Fe(Htrz)₂(trz)] (BF₄) [19,20] are retained with the addition of polyaniline and that the composite can act as a thermal or optical switch. The results of this study also demonstrated that the type of polyaniline (polyaniline 1 or polyaniline 2) plays an important role in the transport properties of the Fe (Htrz)₂(trz)](BF₄) plus polyaniline composite. In terms of obtaining low on state resistance, the combination of Fe(Htrz)2(trz)](BF4) plus polyaniline 1 was better in comparison to the combination of Fe(Htrz)₂(trz)] (BF₄) plus polyaniline 2 as the conductance was higher for Fe (Htrz)₂(trz)](BF₄) plus polyaniline 1 than Fe(Htrz)₂(trz)](BF₄) plus polyaniline 2 (Fig. 2). Synthesis that enables better control of the polyaniline additive is indicated by the better conductance of Fe (Htrz)₂(trz)](BF₄) plus polyaniline 1 than Fe(Htrz)₂(trz)](BF₄) plus polyaniline 2, which was not directly evident from prior work [12], but could be inferred. Additionally, the influence of different factors that could affect the conductance might be controlled by a number of ways such as: i) changing the Fe(Htrz)2(trz)](BF4) to polyaniline ratio, ii) modifying the polyaniline through doping or chain length and iii) changing the thin film deposition technique and solvent, thus changing the molecular arrangement and packing. The results of this study further validate that one route to the problem of high impedance of spin crossover molecules, considered for device applications, would be the addition of other organics like polyaniline [12] and 7,7,8,8-tetracyano-quinodimethane (TCNQ) [46] to increase the conductance.

Author contributions

The manuscript was written through contributions of all authors. All authors have given approval to the final version of the manuscript.

Declaration of competing interest

The authors declare that they have no known competing financial interests or personal relationships that could have appeared to influence the work reported in this paper.

Acknowledgements

This research was supported by the National Science Foundation through NSF-DMR 2003057 [T. K. Ekanayaka, P. A. Dowben], NSF-DMR: 1827690 [R. Y. Lai, K. A. McElveen, E. Mishra] and through EPSCoR RII Track-1: Emergent Quantum Materials and Technologies (EQUATE), Award OIA-2044049 [R. Y. Lai, K. A. McElveen]. The research was performed in part in the Nebraska Nanoscale Facility: National Nanotechnology Coordinated Infrastructure which supported by the National Science Foundation under award no. ECCS: 1542182.

References

- P. Gütlich, A. Hauser, H. Spiering, Thermal and optical switching of iron(II) complexes, Angew Chem. Int. Ed. Engl. 33 (1994) 2024–2054.
- [2] A. Tissot, H.J. Shepherd, L. Toupet, E. Collet, J. Sainton, G. Molnár, P. Guionneau, M.L. Boillot, Temperature- and pressure-induced switching of the molecular spin state of an orthorhombic iron(III) spin-crossover salt, Eur. J. Inorg. Chem. (5–6) (2013) 1001–1008.
- [3] J. Laisney, H.J. Shepherd, L. Rechignat, G. Molnár, E. Rivière, M.L. Boillot, Pressure-induced switching properties of the iron(III) spin-transition complex [FeIII(3-OMeSalEen)₂]PF₆, Phys. Chem. Chem. Phys. 20 (2018) 15951–15959.
- [4] M.G. Cowan, J. Olguín, S. Narayanaswamy, J.L. Tallon, S. Brooker, Reversible switching of a cobalt complex by thermal, pressure, and electrochemical stimuli: abrupt, complete, hysteretic spin crossover, J. Am. Chem. Soc. 134 (2012) 2003–2004.
- [5] B. Warner, J.C. Oberg, T.G. Gill, F. El Hallak, C.F. Hirjibehedin, M. Serri, S. Heutz, M.A. Arrio, P. Sainctavit, M. Mannini, G. Poneti, R. Sessoli, P. Rosa, Temperatureand light-induced spin crossover observed by X-ray spectroscopy on isolated Fe(II) complexes on gold, J. Phys. Chem. Lett. 4 (2013) 1546–1552.
- [6] G.A. Craig, J.S. Costa, O. Roubeau, S.J. Teat, H.J. Shepherd, M. Lopes, G. Molnár, A. Bousseksou, G. Aromí, High-temperature photo-induced switching and pressureinduced transition in a cooperative molecular spin-crossover material, Dalton Trans. 43 (2014) 729–737.
- [7] M. Bernien, H. Naggert, L.M. Arruda, L. Kipgen, F. Nickel, J. Miguel, C. F. Hermanns, A. Krüger, D. Krüger, E. Schierle, E. Weschke, F. Tuczek, W. Kuch, Highly efficient thermal and light-induced spin-state switching of an Fe(II) complex in direct contact with a solid surface, ACS Nano 9 (2015) 8960–8966.
- [8] C. Lefter, R. Tan, J. Dugay, S. Tricard, G. Molnár, L. Salmon, J. Carrey, W. Nicolazzi, A. Rotaru, A. Bousseksou, Unidirectional electric field-induced spinstate switching in spin crossover based microelectronic devices, Chem. Phys. Lett. 644 (2016) 138–141.
- [9] T.K. Ekanayaka, G. Hao, A. Mosey, A.S. Dale, X. Jiang, A.J. Yost, K.R. Sapkota, G. T. Wang, J. Zhang, A.T. N'Diaye, A. Marshall, R. Cheng, A. Naeemi, X. Xu, P. A. Dowben, Nonvolatile voltage controlled molecular spin-state switching for memory applications, Magnetochemistry 7 (2021) 37.
- [10] A. Mosey, A.S. Dale, G. Hao, A. N'Diaye, P.A. Dowben, R. Cheng, Quantitative study of the energy changes in voltage-controlled spin crossover molecular thin films, J. Phys. Chem. Lett. 11 (2020) 8231–8237.
- [11] G. Hao, A. Mosey, X. Jiang, A.J. Yost, K.R. Sapkota, G.T. Wang, X. Zhang, J. Zhang, A.T. N'Diaye, R. Cheng, X. Xu, P.A. Dowben, Nonvolatile voltage controlled molecular spin state switching, Appl. Phys. Lett. 114 (2019), 032901.
- [12] D. Nieto-Castro, F.A. Garcés-Pineda, A. Moneo-Corcuera, I. Sánchez-Molina, J. R. Galán-Mascarós, Mechanochemical processing of highly conducting organic/inorganic composites exhibiting spin crossover-induced memory effect in their transport properties, Adv. Funct. Mater. (2021) 2102469.
 [13] A. Diacontu, S.L. Lupu, I. Rusu, I.M. Risca, L. Salmon, G. Molnár, A. Bousseksou,
- [13] A. Diaconu, S.L. Lupu, I. Rusu, I.M. Risca, L. Salmon, G. Molnár, A. Bousseksou, P. Demont, A. Rotaru, Piezoresistive effect in the [Fe(Htrz)₂(Trz)](BF₄) spin crossover complex, J. Phys. Chem. Lett. 8 (2017) 3147–3151.

- [14] J. Króber, J.-P. Audiére, R. Claude, E. Codjovi, O. Kahn, J.G. Haasnoot, F. Groliere, C. Jay, A. Bousseksou, Spin transitions and thermal hysteresis in the molecular-based materials [Fe(Htrz)₂(Trz)][BF₄) and [Fe(Htrz)₃][BF₄)2-H₂O (Htrz = 1,2,4-4H-triazole; trz = 1,2,4-triazolato), Chem. Mater. 6 (1994) 1404-1412.
- [15] S.A. Siddiqui, O. Domanov, E. Schafler, J. Vejpravova, H. Shiozawa, Synthesis and size-dependent spin crossover of coordination polymer [Fe(Htrz)₂(Trz)](BF₄), J. Mater. Chem. C 9 (2021) 1077–1084.
- [16] A. Grosjean, P. Négrier, P. Bordet, C. Etrillard, D. Mondieig, S. Pechev, E. Lebraud, J.F. Létard, P. Guionneau, Crystal structures and spin crossover in the polymeric material [Fe(Htrz)₂(trz)](BF₄) including coherent-domain size reduction effects, Eur. J. Inorg. Chem. 2013 (2013) 796–802.
- [17] A. Grosjean, N. Daro, S. Pechev, C. Etrillard, G. Chastanet, P. Guionneau, Crystallinity and microstructural versatility in the spin-crossover polymeric material [Fe(Htrz)₂(Trz)](BF₄), Eur. J. Inorg. Chem. (2018) 429–434.
- [18] A. Urakawa, W. Van Beek, M. Monrabal-Capilla, J.R. Galán-Mascarós, L. Palin, M. Milanesio, Combined, modulation enhanced X-ray powder diffraction and Raman spectroscopic study of structural transitions in the spin crossover material [Fe(Htrz)₂(trz)](BF₄), J. Phys. Chem. C 115 (2011) 1323–1329.
- [19] C. Lefter, I.A. Gural'skiy, H. Peng, G. Molnár, L. Salmon, A. Rotaru, A. Bousseksou, P. Demont, Dielectric and charge transport properties of the spin crossover complex [Fe(Htrz)₂(Trz)](BF₄), Phys. Status Solidi Rapid Res. Lett. 8 (2014) 191–193.
- [20] A. Rotaru, I.A. Gural'skiy, G. Molnár, L. Salmon, P. Demont, A. Bousseksou, Spin state dependence of electrical conductivity of spin crossover materials, Chem. Commun. 48 (2012) 4163–4165.
- [21] C. Etrillard, V. Faramarzi, J.-F. Dayen, J.F. Letard, B. Doudin, Photoconduction in [Fe(Htrz)₂(trz)](BF₄)-H₂O nanocrystals, Chem. Commun. 47 (2011) 9663–9665.
- [22] D. Tanaka, N. Aketa, H. Tanaka, S. Horike, M. Fukumori, T. Tamaki, T. Inose, T. Akai, H. Toyama, O. Sakata, H. Tajirig, T. Ogawa, Facile preparation of hybrid thin films composed of spin-crossover nanoparticles and carbon nanotubes for electrical memory devices, Dalton Trans. 48 (2019) 7074–7079.
- [23] F. Prins, M. Monrabal-Capilla, E.A. Osorio, E. Coronado, H.S.J. van der Zant, Room-temperature electrical addressing of a bistable spin-crossover molecular system, Adv. Mater. 23 (2011) 1545–1549.
- [24] H.O. Jeschke, L.A. Salguero, B. Rahaman, C. Buchsbaum, V. Pashchenko, M. U. Schmidt, T. Saha-Dasgupta, R. Valentí, Microscopic modeling of a spin crossover transition, New J. Phys. 9 (2007) 448.
- [25] Y.-C. Chen, Y. Meng, Z.-P. Ni, M.-L. Tong, Synergistic electrical bistability in a conductive spin crossover heterostructure, J. Mater. Chem. C 3 (2015) 945.
- [26] V.G. Kulkarni, Processing of polyanilines, in: M. Aldissi (Ed.), Intrinsically Conducting Polymers: an Emerging Technology, NATO ASI Series (Series E: Applied Sciences), vol. 246, Springer, Dordrecht, 1993, pp. 45–50, https://doi.org/ 10.1007/978-94-017-1952-0 5.
- [27] S.M. Hammo, Effect of acidic dopant properties on the electrical conductivity of polyaniline, Tikrit J. Pure Sci. 17 (2012) 6–10.
- [28] J.-C. Chiang, A.G. MacDiarmid, 'Polyaniline': protonic acid doping of the emeraldine form to the metallic regime, Synth. Met. 13 (1986) 193–205, https:// doi.org/10.1016/0379-6779(86)90070-6.
- [29] F. Usman, J.O. Dennis, A.Y. Ahmed, K.C. Seong, Y.W. Fen, A.R. Sadrolhosseini, F. Meriaudeau, P. Kumar, O.B. Ayodele, Structural Characterization and optical constants of p-toluene sulfonic acid doped polyaniline and its composites of chitosan and reduced graphene oxide, J. Mater. Res. Technol. 9 (2020) 1468–1476.
- [30] S.J. Tang, A.T. Wang, S.Y. Lin, K.Y. Huang, C.C. Yang, J.M. Yeh, K.C. Chiu, Polymerization of aniline under various concentrations of APS and HCl, Polym. J. 43 (2011) 667–675.
- [31] S. Sinha, S. Bhadra, D. Khastgir, Effect of dopant type on the properties of polyaniline, J. Appl. Polym. Sci. 112 (2009) 3135–3140.
- [32] M.V. Kulkarni, A.K. Viswanath, R.C. Aiyer, P.K. Khanna, Synthesis, characterization, and morphology of p-toluene sulfonic acid-doped polyaniline: a material for humidity sensing application, J. Polym. Sci., Part B: Polym. Phys. 43 (2005) 2161–2169.
- [33] J.C. Chiang, A.G. MacDiarmid, Polyaniline": protonic acid doping of the emeraldine form to the metallic regime, Synth. Met. 13 (1986) 193–205.
- [34] G. D'Aprano, M. Leclerc, G. Zotti, Stabilization and characterization of pernigraniline salt: the "acid-doped" form of fully oxidized polyanilines, Macromolecules 25 (1992) 2145–2150.
- [35] A. Rahy, D.J. Yang, Synthesis of highly conductive polyaniline nanofibers, Mater. Lett. 62 (2008) 4311–4314.
- [36] S. Kamarudin, M.S.A. Rani, M. Mohammad, N.H. Mohammed, M.S. Su'ait, M. A. Ibrahim, N. Asim, H. Razali, Investigation on size and conductivity of polyaniline nanofiber synthesised by surfactant-free polymerization, J. Mater. Res. Technol. 14 (2021) 255–261.
- [37] T. Mahfoud, G. Molnár, S. Cobo, L. Salmon, C. Thibault, C. Vieu, P. Demont, A. Bousseksou, Electrical properties and non-volatile memory effect of the [Fe(HB (Pz)₃)₂] spin crossover complex integrated in a microelectrode device, Appl. Phys. Lett. 99 (2011) 157.
- [38] G. Kalon, Y. Jun Shin, V. Giang Truong, A. Kalitsov, H. Yang, The role of charge traps in inducing hysteresis: capacitance-voltage measurements on top gated bilayer graphene, Appl. Phys. Lett. 99 (2011), 083109.
- [39] E. Echeverria, B. Dong, G. Peterson, J.P. Silva, E.R. Wilson, M.S. Driver, Y.S. Jun, G.D. Stucky, S. Knight, T. Hofmann, Z.K. Han, N. Shao, Y. Gao, W.N. Mei, M. Nastasi, P.A. Dowben, J.A. Kelber, Semiconducting boron carbides with better charge extraction through the addition of pyridine moieties, J. Phys. D Appl. Phys. 49 (2016) 355302.
- [40] G.G. Peterson, E. Echeverria, B. Dong, J.P. Silva, E.R. Wilson, J.A. Kelber, M. Nastasi, P.A. Dowben, Increased drift carrier lifetime in semiconducting boron

- carbides deposited by plasma enhanced chemical vapor deposition from carboranes and benzene, J. Vac. Sci. Technol. A Vacuum, Surfaces, Film. 35 (2017), 03E101.
- [41] A. Oyelade, A.J. Yost, N. Benker, B. Dong, S. Knight, M. Schubert, P.A. Dowben, J. A. Kelber, Composition-dependent charge transport in boron carbides alloyed with aromatics: plasma enhanced chemical vapor deposition aniline/orthocarborane films, Langmuir 34 (2018) 12007–12016.
- [42] A. Oyelade, A. Osonkie, A.J. Yost, N. Benker, P.A. Dowben, J.A. Kelber, Optical, electronic and visible-range photo-electronic properties of boron carbide-indole films, J. Phys. D Appl. Phys. 53 (2020) 355101.
- [43] C.C. Ilie, F. Guzman, B.L. Swanson, I.R. Evans, P.S. Costa, J.D. Teeter, M. Shekhirev, N. Benker, S. Sikich, A. Enders, P.A. Dowben, A. Sinitskii, A.J. Yost,
- Inkjet printable-photoactive all inorganic perovskite films with long effective photocarrier lifetimes, J. Phys. Condens. Matter 30 (2018) 18LT02.
- [44] Z.G. Marzouk, A. Dhingra, Y. Burak, V. Adamiv, I. Teslyuk, P.A. Dowben, Long carrier lifetimes in crystalline lithium tetraborate, Mater. Lett. 297 (2021) 129978.
- [45] G.G. Peterson, Q. Su, Y. Wang, N.J. Ianno, P.A. Dowben, M. Nastasi, Improved a -B₁₀C_{2+x}H_y/Si p-n heterojunction performance after neutron irradiation, J. Vac. Sci. Technol. B, Nanotechnol. Microelectron. Mater. Process. Meas. Phenom. 36 (2018), 011207.
- [46] Ö. Ungör, E.S. Choi, M. Shatruk, Optimization of crystal packing in semiconducting spin-crossover materials with fractionally charged TCNQ $^{\delta}$ anions (0 < δ < 1), Chem. Sci. 12 (2021) 10765–10779.
- [47] C. Lan, C. Li, Y. Yin, Y. Liu, Large-area synthesis of monolayer WS2 and its ambient-sensitive photo-detecting performance, Nanoscale 7 (2015) 5974–5980.